Polymer Brush−GaAs Interface and Its Use as an Antibody-Compatible Platform for Biosensing

Daniela T. Marquez, Juliana Chawich, Walid M. Hassen, Khalid Moumanis, Maria C. DeRosa,*
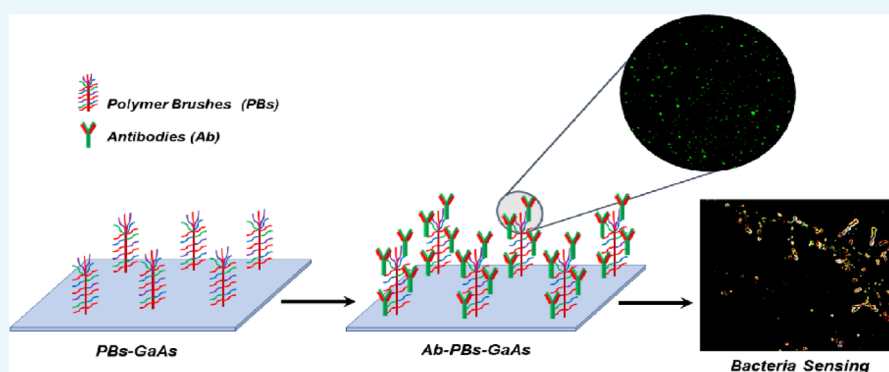and Jan J. Dubowski*

ACCESS | Metrics & More | Article Recommendations | Supporting Information

ABSTRACT: Despite evidence showing that polymer brushes (PBs) are a powerful tool used in biosensing for minimizing nonspecific interactions, allowing for optimization of biosensing performance, and the fact that GaAs semiconductors have proven to have a remarkable potential for sensitive biomolecule detection, the combination of these two robust components has never been considered nor evaluated as a platform for biosensing applications. This work reports different methodologies to prepare and tune PBs on the GaAs interface (PB−GaAs) and their potential as useful platforms for antibody grafting, with the ultimate goal of demonstrating the innovative and attractive character of the PB−GaAs interfaces in the enhanced capture of antibodies and control of nonspecific interactions. Three different functionalization approaches were explored, one "grafting-to" and two "grafting-from," in which atom transfer radical polymerization (ATRP) was performed, followed by their corresponding characterizations. Demonstration of the compatibility of *Escherichia coli* (*E. coli*) and *Legionella pneumophila* (*Lp*) antibodies with the PB−GaAs platform compared to the results obtained with conventional biosensing architectures developed for GaAs indicates the attractive potential for operation of a sensitive biosensor. Furthermore, these results showed that by carefully choosing the nature and preparation methodology of a PB−GaAs interface, it is possible to effectively tune the affinity of PB−GaAs-based sensors toward *E. coli* and *Lp* antibodies ultimately demonstrating the superior specificity of the developed biosensing platform.

1. INTRODUCTION

In the past few decades, substantial efforts have been made to unravel the structural details related to the modification and control of surface properties of various organically functionalized materials. The proper understanding and control of self-assembled monolayers (SAMs) have been crucial for the development of useful molecular electronic devices, allowing for significant advances in the field of biosensors and surface science and prompting the successful development, growth, and incorporation of polymer brushes (PBs) on a variety of supporting substrates.

Pathogenic bacteria detection using biosensors remains a rich subject explored by researchers, and many tools have been reported using different transducers such as surface plasmon resonance, electrochemical impedance spectroscopy, fiber optics, and piezoelectric devices.[1]

Recently, GaAs semiconductors have been recognized as a platform compatible with acoustic and photoluminescence biosensing techniques, demonstrating a remarkable potential for sensitive biomolecule detection.[2−4] The high sensitivity of GaAs' photoluminescence, associated mostly with surface changes, opens the door for further biosensor improvement and the possibility of even higher sensitivities achieved by fabricating innovative biosensors and delivering sensitive analysis at attractive costs. Furthermore, photoluminescence-
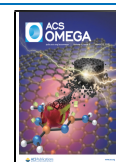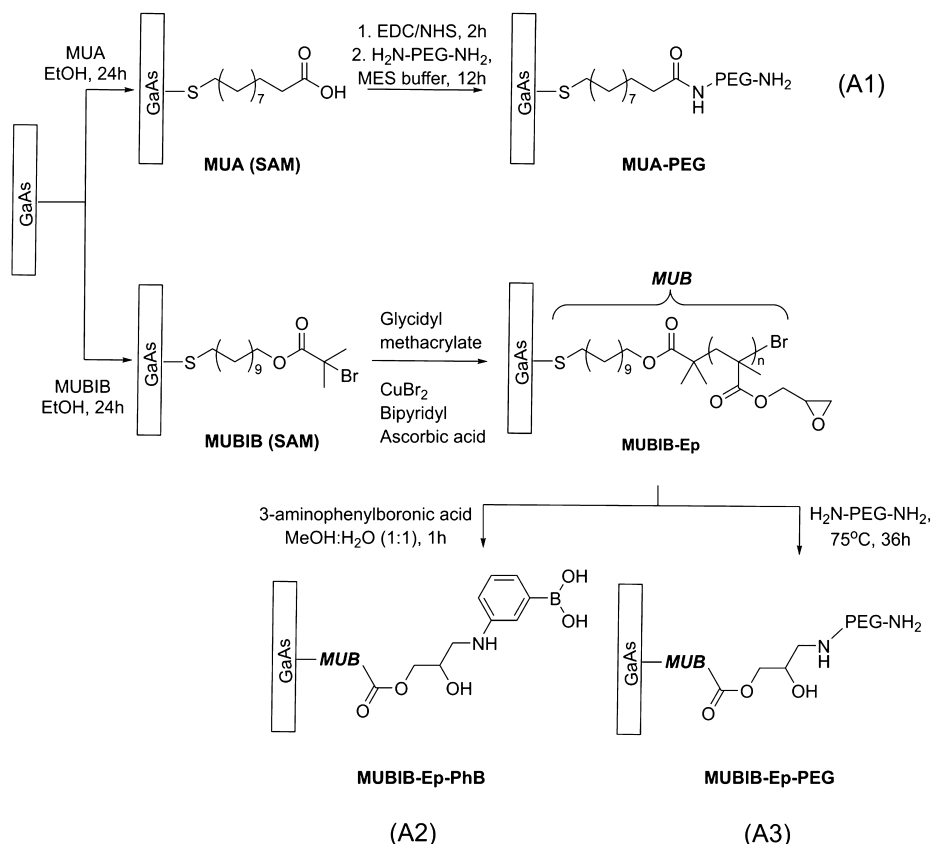
Scheme 1. Graphical Representation of SAM Formation on GaAs Followed by Polymer Brush Formation Through the "Grafting-to" Approach (A1), Phenylboronic Acid "Grafting-From" Approach (A2), and Poly(ethylene)glycol "Grafting-From" Approach (A3)

based biosensors using GaAs/AlGaAs nanoheterostructure biochips consisting of conventionally thiolated SAM architectures and functionalized with antibodies were reported to be capable of detecting *Escherichia coli (E.coli)* and *Legionella pneumophila* (Lp) ssp1 at concentrations as low as 10^3 CFU/mL.[2,4,5]

The three-dimensional character of PBs combined with the vast possibilities of modifying functional groups has positioned them as a powerful strategy to minimize nonspecific interactions, leading to optimized biosensing performance and considerable improvements in the limits of detection.[6−8] Moreover, PB semiconductor surfaces such as silicon, silicon carbide, and graphene substrates[9−11] have attracted considerable attention because of the unique semiconductor surface properties, resulting in several incorporation strategies being developed to facilitate manufacturing protocols while improving the biosensors' performance.[12−15]

Surprisingly, although important findings related to the formation and characterization of SAMs on GaAs substrates have been reported,[16,17] the incorporation of PBs on GaAs and the characterization of such an interface is a scarcely investigated field. Even more, in spite of the fact that PBs have proven to have a significant positive impact in biosensing performance, while GaAs semiconductors have demonstrated to have considerable potential in biomolecule sensing, the combination of these two powerful tools and its evaluation as a platform for biosensing applications has never been explored.

In this work, we have evaluated—to the best of our knowledge—for the first time the potential of PB structures on GaAs (PB−GaAs) as a platform for biosensing applications. As

a main approach, we have focused on developing methodologies and tuning the PB−GaAs interface to enhance capture of antibodies and control nonspecific interactions necessary for the specific capture of *E. coli* and *L. pneumophila*. PBs were grown on GaAs (001) substrates followed by their corresponding thorough characterization. The compatibility between PB−GaAs and IgG-anti-*E. coli* and *L. pneumophila* antibodies, acting as target recognition agents, was further assessed.

Three different approaches to grow PBs on GaAs were evaluated, namely, "grafting-to" (A1), "grafting-from" (A2), and a modified version of the latter (A3). As shown in Scheme 1, A1 consists of a 11-mercaptoundecanoic acid (MUA) SAM formed on the surface of GaAs, to which poly(ethylene glycol) diamine (PEG) is further grafted. On the other hand, A2 and A3 consist of the initial formation of a mercaptoundecyl bromoisobutyrate (MUBIB) initiator SAM, to which the glycidyl methacrylate (GMA) monomer is polymerized through atom transfer radical polymerization (ATRP). Further modifications with either phenylboronic acid or PEG give rise to approaches A2 and A3, respectively; the incorporated moieties will serve as the future link for antibody grafting.

2. RESULTS AND DISCUSSION

2.1. Characterization of PBs on GaAs. Formation of SAMs is a fundamental step in the successful growth of PBs. In the case of GaAs, SAM semiconductor interfaces are known to be formed through covalent bonding between thiolated species and the GaAs surface via GaAs−S bonds.[18,19] Figure 1 shows
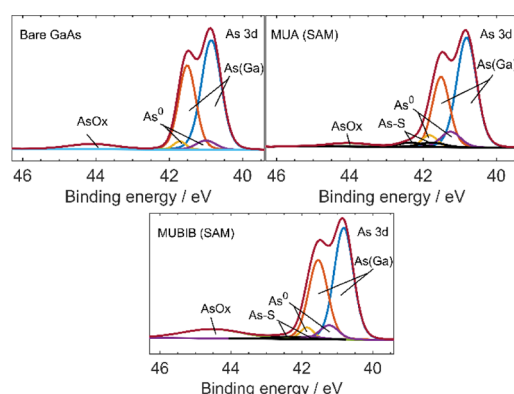
Figure 1. XPS As 3d peak analysis of bare GaAs (top left), MUA SAM (top right), and MUBIB SAM (bottom) on GaAs, respectively. Note: Less intense signals are expected because of the SAM nature of the samples analyzed through this technique.

the As 3d core-level X-ray photoelectron spectroscopy (XPS) spectra corresponding to bare GaAs, MUBIB (SAM), and MUA (SAM). Covalent bonding of both MUBIB and MUA to GaAs was confirmed through the deconvolution of As 3d XPS peaks; a doublet peak additional to those corresponding to elemental As and As(Ga), centered at ~42.4 eV, was identified as As−S, while this doublet was absent in the case of bare GaAs. As expected, these values agreed with the literature for thiol-based SAMs.[20,21] Unfortunately, obtaining clear XPS spectra of the built PBs samples was not feasible because of overcrowded signals. However, PBs characterization was achieved by complementing the other techniques such as FTIR, AFM, contact angle, and ellipsometry.

The thickness corresponding to each step involved in PBs formation for the three approaches studied in this work was determined by ellipsometry (see Table 1). MUBIB (ATRP initiator) SAM—a common step in the preparation of A2 and A3—had a final thickness of approximately 2 nm upon incubation of GaAs in MUBIB for 24 h. After 24 h incubation, most SAMs reach their maximum packing capability upon binding to the surface in the first few hours followed by slow

Table 1. PBs Thickness and Polymer Loading for Samples Obtained in Each Step of the Studied Approaches

sample	film thickness[a] [nm]	polymer loading[b] [ng mm^{-2}]	description
MUA−SAM	7.50 ± 0.57	9.01	24 h incubation
MUBIB−SAM	~2	~2.4	24 h incubation
MUA−PEG-50	11.8 ± 0.87	14.2	50 mg/mL PEG
MUA−PEG-100	12.8 ± 0.56	15.4	100 mg/mL PEG
MUBIB−Ep2	17.8 ± 0.89	21.3	2 h ATRP
MUBIB−Ep8	42.5 ± 0.26	50.9	8 h ATRP
MUBIB−Ep2−PhB	22.8 ± 0.34	27.4	2 h ATRP
MUBIB−Ep8−PhB	46.5 ± 1.32	55.8	8 h ATRP
MUBIB−Ep2−PEG	32.6 ± 2.68	39.2	2 h ATRP
MUBIB−Ep8−PEG	30.1 ± 2.85	37.1	8 h ATRP

[a]Determined from ellipsometry measurements. [b]Determined from thickness assuming a density of 1.2 g/cm^3 corresponding to the refractive index of 1.5 for all compounds.

re-organization and packing; values of ~2 nm are common for most SAMs on GaAs.[13,19]

The thicknesses obtained for MUBIB−Ep PBs upon ATRP (A2 and A3) were tunable. As expected, longer polymerization times gave rise to thicker structures; PBs with double the thickness were achieved by varying the polymerization times from 2 h (MUBIB−Ep2) to 8 h (MUBIB−Ep8). Similar MUBIB (SAM) thicknesses were found when comparing the results for GaAs obtained in this study with those found in the literature for the same type of PBs on gold substrates;[22] however, thicker PBs were reported for the latter upon ATRP incorporation. This discrepancy is mostly likely due to the differences in the nature of the substrates to be functionalized, causing variations in the level of organization and/or affinity between SAMs on gold versus GaAs which in turn translate directly into the differences brought by this work regarding the functionalization of GaAs compared to the known methods applied for glass, Au, and other substrates. For example, it has been previously described that lower fractions of initiator (MUBIB) on the substrate's surface give rise to thinner PBs.[23] In the case of our substrate, the prolonged exposure to a water-containing environment during the formation of the MUBIB−Ep structure will induce a certain degree of dark corrosion in GaAs[24] —a phenomenon absent in the case of Au and glass substrates—giving rise to a reduced initiator fraction concomitantly decreasing the rate of MUBIB deposition and producing thinner SAMs. Although the presence of water could have a detrimental effect on the quality of the GaAs substrate, previous experiments related to 16-mercaptohexadecanoic acid SAM deposition on GaAs in the presence of water (RT, 20 h) suggested that water helps produce enhanced quality SAMs.[20,25]

Upon further incorporation of phenylboronic acid moieties (A2), the thickness of the PBs increased by approximately 5 nm regardless of the polymerization time in the previous step. Nevertheless, when PEG diamine was grafted instead of phenylboronic acid, similar thicknesses were obtained independent of the ATRP time. This can be attributed to the experimental conditions involved in approach A3, such as higher temperatures (75 °C) and longer exposure times (36 h), when PEG chains are grafted. Higher temperatures would allow for better access of the PEG chains to the epoxide groups in the MUBIB−Ep PBs which, upon cooling, may produce a more compact brush compared to those obtained when incorporating groups at room temperature (as in the case of A2). This statement is supported by previous publications on the dependence of PEG PBs with temperature indicating that PEG chains can reach a fully collapsed state above 35 °C.[26]

Finally, MUA−SAM formed in the A1 approach is thicker compared to MUBIB SAM. This could be attributed to the bulkier head groups of the latter that could lead to a less packed SAM impacting monolayer average thickness.[27]

Visual evidence of PBs formation as well as roughness factors were obtained through AFM topographical images (shown in Figure 2). These results were further complemented by performing FTIR spectroscopy to confirm the presence of the expected end functional groups (Figure 3).

FTIR was performed on the different samples to confirm the successful grafting of PBs and the presence of the functional groups needed for further antibody attachment. Figure 3 (top, left) shows the FTIR spectra for the A2 approach where (a) corresponds to MUBIB−Ep and (b) to MUBIB−Ep−PhB. As it can be seen, spectrum (b) maintains most of the peaks
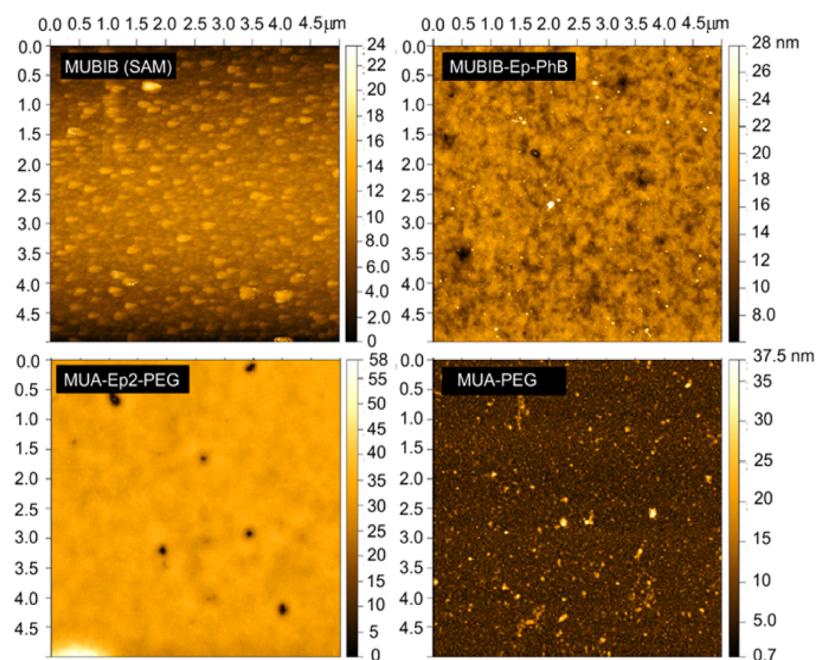
Figure 2. AFM images of MUBIB−SAM (top left, σ_{RMS} = 2.52), MUBIB−Ep−PhB (top right, σ_{RMS} = 1.74), MUBIB−Ep2−PEG (bottom left, σ_{RMS} = 2.58), and A−MUA−PEG (bottom right, σ_{RMS} = 6.08). Note: Different scale bars were purposely selected for visual aid.
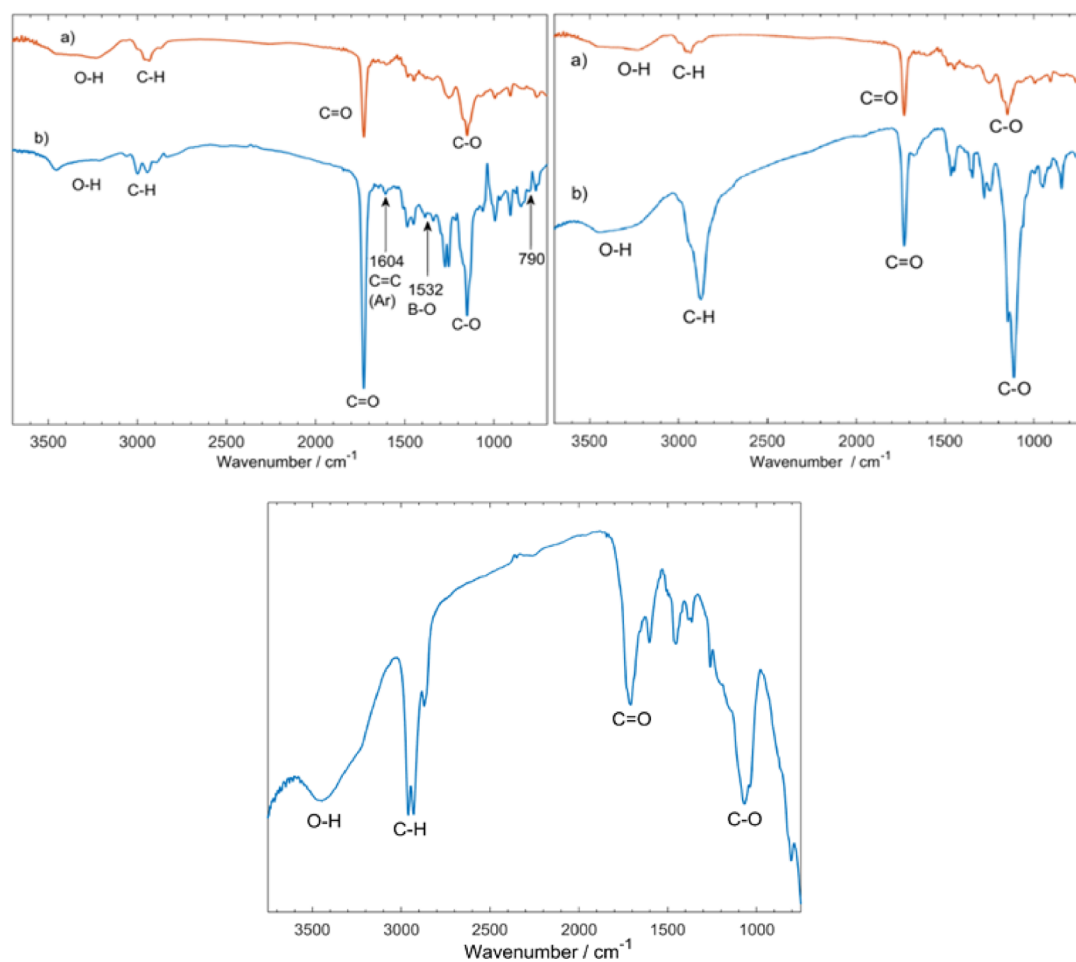

Figure 3. FTIR spectra corresponding to (top, left) approach A2, MUBIB−Ep (a), and MUBIB−Ep−PhB (b), (top, right) A3, MUBIB−Ep−PEG (a) and MUBIB−Ep−PEG (b), and (bottom) approach A1 (MUA−PEG).

present in spectrum (a) besides having additional ones corresponding to A2. The band at 1352 cm^{-1} has been previously assigned to B−O stretching,[28,29] while the bands at 1604 and 1581 cm^{-1} correspond to the C=C stretching of the benzene ring. In addition, the band at 790 cm^{-1} can be attributed to the 1,3-disubstituted benzene. These results confirm the successful conjugation of phenylboronic acid to MUBIB−Ep. A similar situation was observed for approaches A3 (top, right) and A1 (bottom), where PEG bands were predominant and intensified the already existing peaks, confirming a successful PEG grafting.

Hydrophobicity is an important parameter to evaluate while building and characterizing PBs, especially when developing biosensors based on PBs−GaAs, where the main goal is specifically to enhance antibody and bacterial capture while reducing nonspecific adsorption. Hence, the contact angle is a relevant parameter to consider when assessing potential in biosensing applications because this factor would influence target detection. It has been previously reported that slightly greater contact angles (higher hydrophobicity) enhance bacterial adhesion as well as detection; typical contact angle values associated with an efficient bacteria detection commonly range from 50 to 70°.[28,29]

Table 2 shows the contact angle and roughness values obtained for the main steps involved in the three studied

Table 2. Contact Angles and σ_{RMS} Values for Main Samples

sample	contact angle (deg)	σ_{RMS} [nm][a]
bare GaAs	74.9 ± 2.19	0.84
MUA−SAM	70.3 ± 0.85	1.98
A−MUA−PEG	63.0 ± 3.28	6.08
B−MUA−PEG	67.9 ± 1.3	2.97
MUBIB−SAM	72.1 ± 3.46	2.52
MUBIB−Ep2	59.8 ± 1.69	2.68
MUBIB−Ep2−PhB	62.8 ± 0.85	1.74
MUBIB−Ep2−PEG	55.7 ± 2.12	2.58

[a]Determined from AFM images.

approaches. A decrease in the contact angle upon final PBs formation, with respect to their corresponding original SAM, was observed, which is consistent with the nature of the end functional groups in each approach. PEG moieties incorporated for A1 and A3 approaches are responsible for a decrease in the contact angle, while the decrease obtained upon phenylboronic acid incorporation can be attributed to the double hydroxyl groups.[30] Despite that, an increase in hydrophobicity is associated with better bacteria adhesion/ detection, and the obtained contact angles fall within the abovementioned range of values associated with an efficient

bacteria adhesion. Furthermore, a slight increase in hydrophilicity has shown to efficiently prevent nonspecific adsorption.[31]

Biosensor surface roughness also plays a relevant role in determining target/antigen recognition−agent interactions. Generally, irregular surfaces promote the interaction with the target because of the greater surface area.[32] As expected, an increase in roughness was observed upon PBs incorporation compared to bare GaAs. PEG grafting for either approach A1 (method B) or A3 seem to have had the same effect in terms of the final roughness, while the incorporation of phenylboronic acid in A2 gave rise to smoother brushes. Particularly higher roughness values, such as that obtained for A−MUA−PEG PBs prepared as indicated in Section 4.2.3., signal a very irregular PBs surface which could potentially affect the outcome in bacteria capture. It is worth mentioning that a consistent decrease in the contact angle with an increase in roughness is observed. As expected, all the surfaces studied are wettable by the solvent used. Hence, a higher surface roughness will have, as a consequence, a higher wettability concomitantly decreasing contact angle value. With the purpose of obtaining MUA-based PBs with a roughness factor comparable to the other approaches included in this study, we implemented method B, prepared as shown in Section 4.2.4. As it can be seen from the AFM images (shown in Figure 4), the PBs prepared through method B gave rise to a much smoother surface. The changes incorporated in method B seem to be sufficient to obtain a smooth brush surface comparable to the other approaches. The first modification involved changing the EDC amine coupling solution concentration (from 0.6 to 0.4 M) and the medium (from MES buffer to deionized water), while the second modification implemented is related to the use of a diamino-PEG solution in DMF rather than incorporating the PEG moieties using MES buffer (pH 4.7). Although a low pH has been previously reported in the literature as a way of activating carboxylic groups when coupling amines and carboxylic groups,[33] other references suggest that pH 7.4 is optimum when performing EDC/NHS coupling. In the case of our PBs, the latter gave rise to smoother brushes. On the other hand, by dissolving diamino-PEG in DMF rather than MES buffer also positively affected the PB's roughness factor, which could be attributed to an improved diamino-PEG solubility at the time of its incorporation. A table summarizing the details of PBs methodologies employed in this work and those applied by others mentioned in this section has been included in the Supporting Information (Table S1) with the aim to provide a useful reference to the technology of GaAs-based biosensors and PB−GaAs interface, as well as to ease a comparison with
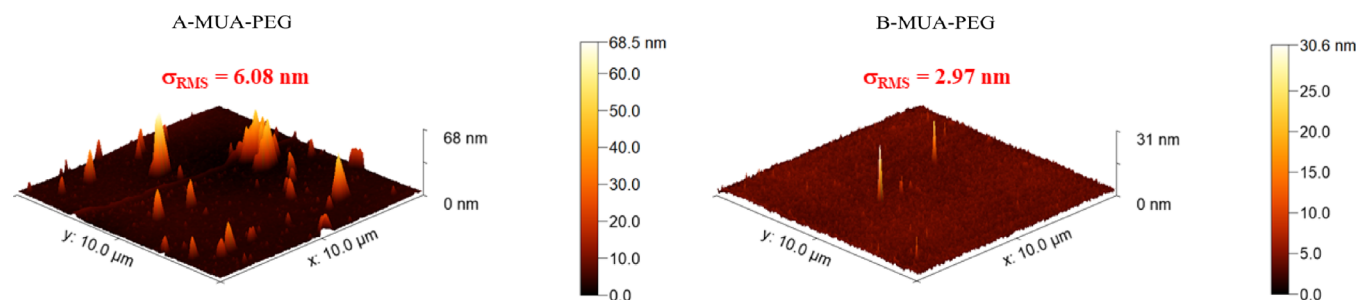

Figure 4. AFM images of A−MUA−PEG (left) and B−MUA−PEG (right). Note: Different Z-axis scales were purposely selected for visual aid.

Table 3. IgG-Anti *E. coli* and IgG-Anti *L. pneumophila* Antibody Surface Coverage

sample	IgG-Anti *E. coli* surface coverage (Ab/mm²)	*E. coli* CV[a] (%)	IgG-Anti *L. pneumophila* surface coverage (Ab/mm²)	*L. pneumophila* CV[a] (%)
MUA−-PEG	10514 ± 2047 (A-A1)	19	174.6 ± 54.7 (A-A1)	30
			401.2 ± 293.8 (B-A1)	73
MUBIB−-Ep−-PhB	321.6 ± 80.32 (A2)	25	5042 ± 1872 (A2)	37
MUBIB−-Ep−-PEG	5418 ± 1685 (A3)	31	5566 ± 939.4 (A3)	17

[a]Intersample coefficient of variation.

PBs interfaces using other substrates. The effect of such modifications in antibody capture can also be appreciated in Section 2.2 in this work.

2.2. Fluorescence Microscopy Antibody Compatibility Assessment. Efficient coupling of the recognition molecules to the PBs surface is imperative to develop sensors that have improved sensitivity and selectivity. Thus, when evaluating if the PB−GaAs combination is suitable for sensing applications, such coupling must be verified.

Table 3 shows the antibody surface coverage results for the three approaches considered in this study for both *E. coli* and *L. pneumophila* obtained upon incubation of PB−GaAs in IgG-anti *L. pneumophila* and IgG-anti *E. coli* antibodies. As it can be seen, in the case of *L. pneumophila* antibodies, the modifications implemented in method B-A1 show a higher antibody surface coverage compared to method A-A1. It is worth mentioning that no evidence of antibody capture was observed in the case of bare GaAs and SAM−GaAs, in contrast with that obtained after treating PB−GaAs with antibodies, confirming the compatibility of the former with such target recognition agents.

As expected, the antibody surface coverage values achieved for each approach were respectable and sufficient to confirm the compatibility of PB−GaAs platform toward IgG-anti *L. pneumophila* and IgG-anti *E. coli*. When capturing IgG-anti *E. coli* antibodies, approaches A1 and A3 proved to be more efficient in contrast to approach A2. On the other hand, approaches A2 and A3 gave rise to considerably higher antibody surface coverage values in the case of *L. pneumophila* compared to approach A1. These differences can be attributed to the PBs structure and show that epoxy/PEG-based PBs favor the capture of both types of antibodies and MUBIB−Ep−PhB-based PBs are more specific for *L. pneumophila* antibodies, while MUA−PEG-based PBs are more specific for *E. coli* antibody capture. These results, although simple, constitute a proof that by tuning the PB−GaAs interface, it is possible to control the specificity of a biosensor. By modifying the nature of the PB−GaAs interface, it is likely possible to affect the spatial disposition and availability of the end functional groups that will ultimately interact with the corresponding antibodies.

The approaches incorporated in this study have advantages and disadvantages that will depend on the user's goal. The A1 approach has a shorter preparation time (total of 22 h) and a simpler preparation methodology, it is less expensive, and it is more specific toward *E. coli* antibodies. On the other hand, the A2 approach has a similar preparation time compared to A1, and although it could be more expensive, with the preparation procedure considered less simpler, its specificity toward *L. pneumophila* antibodies is significantly greater than that of the other approaches. Finally, the preparation of A3 takes 36 more hours than that of A1 and A2. However, it would be less

expensive and more useful when a generic sensing platform is needed.

When comparing coefficients of variation for different approaches, it has been observed that the homogeneity in antibody distribution varied from case to case. From these results, it is not possible to conclude unequivocally a correlation between antibody distribution and sensor specificity encouraging the further future investigation related to this aspect. Nevertheless, MUA−PEG indicating more than 10 times greater coverage for *E. coli* than for *L. pneumophila* antibodies may be related to the less discriminated deposition of *E. coli* antibodies on such structures.

Preliminary bacteria capture experiments were performed to confirm antibody-PB−GaAs compatibility and corroborate that the practical detection of bacteria is, in fact, feasible. The number of attached bacteria is sufficient to confirm the feasibility of using PBs−GaAs as a platform for bacteria capture. Table S2 presents the number of captured *E. coli* per mm² for the different investigated architectures following the exposure of functionalized GaAs chips to two bacterial suspensions at concentrations of 10³ and 10⁵ CFU/mL. The obtained coverage is two to three times higher than what it was reported for conventional architecture based on SAM thiol-neutravidin−biotinylated antibody reported by Aziziyan et al.[34] Moreover, the average bacteria coverage values of the PBs−GaAs were found to be around 100 bacteria/mm² at the tested incubation concentrations of 10³ CFU/mL, which compares to what has been previously reported for GaAs biosensors coupled with other sensitive detection techniques.[2,3,35]

Photoluminescence-based biosensors using GaAs/AlGaAs nanoheterostructure biochips consisting of conventionally thiolated antibody-functionalized SAM architectures were reported to be capable of detecting bacteria by monitoring the change in rate of digital photocorrosion in the presence of Gram-negative bacteria.[2,4,5] Its multilayered character has positioned GaAs/AlGaAs biochips as excellent candidates for re-functionalization. Upon photocorrosion of the outer layer, a clean new layer is exposed and is ready to be functionalized, allowing us to perform several measurements using the same biochip. However, in order to obtain automated re-functionalization devices for remote sensing, it is of key importance to count with functionalization methodologies compatible with remote automation.

The simplicity of the methodologies for the preparation of PB−GaAs presented herein, which involve the incubation of substrates in premade solutions, and the fact that most steps are performed at room temperature constitute an added value to these platforms because it renders them as suitable for automated re-functionalization of devices designed for remote sensing.

3. CONCLUSIONS

We have investigated different methodologies to prepare PBs on GaAs and demonstrated their promising potential as antibody-compatible platforms for biosensing, as well as the innovative and attractive character of controlling the PB–GaAs interface in order to enhance antibody capture and control nonspecific interactions. By carefully selecting the nature of the PB–GaAs interface and the right fabrication methodology, it is possible to control the specificity of such sensing platforms toward the tested antibodies.

The successful growth of PBs on GaAs suggests a significant versatility of this interface in terms of its chemical and physical properties, which, combined with its compatibility with different antibodies, makes PB–GaAs a useful platform for biosensing applications. We have incorporated both *E. coli* and *L. pneumophila* antibodies to this system through tunable functional groups, highlighting the possibility of developing sensors able to target other bacteria and bio-architectures. A thorough characterization of each structure and a comparison with previously published procedures for PBs fabrication have pointed out the importance of implementing procedures dedicated specifically to GaAs, compared to those applied for functionalization of the alternative biosensor substrates. Furthermore, the employed functionalization methodology poses PB–GaAs as an excellent platform compatible with automated re-functionalization for remote sensing.

4. MATERIALS AND METHODS

4.1. Materials. 11-mercapto-1-undecanol (MUDO, 97%), α-bromoisobutyryl bromide (98%), ammonium chloride, dichloromethane (anhydrous, ≥99.8%), diethyl ether, 4-dimethylaminopyridine, 2-N,N'-(dimethylamino)ethyl metacrylate (98%), copper (II) bromide (CuBr$_2$, 99.999%), 2,2'-bipyridyl (>99%), *N,N*-dimethylformamide (DMF), ethanolamine hydrochloride, GMA (97%), hexane (anhydrous, 95%), L-ascorbic acid, 3-aminophenylboronic acid, lysogeny broth (LB), magnesium sulfate, phosphate buffered saline (PBS) solution (10×, pH 7.4), PEG diamine (Mn 2000), pyridine (99.8%), toluene, and triethylamine were purchased from Sigma-Aldrich (Oakville, Canada) and used without further purification.

N-(3-dimethylaminopropyl)-*N'*-ethylcarbodiimide hydrochloride (EDC) and *N*-hydroxysuccinimide (NHS) used for activation were prepared from an amine coupling kit purchased from GE Healthcare Canada (Mississauga, Canada).

Semiconductor-grade OptiClear (National Diagnostics, USA), acetone (ACP Chemicals, Canada), anhydrous ethanol (Brampton, Canada), ammonium hydroxide (28%, Anachemia, Canada), isopropyl alcohol (2-propanol, Fisher Scientific (Ottawa, Canada), and methanol (VWR Chemicals, Canada) were used.

Unconjugated polyclonal antibodies against *E. coli* and *L. pneumophila* were obtained from Virostat, Inc. (Portland, Marine). Aqueous solutions were prepared using 18.2 MΩ cm^{-1} Milli-Q water obtained from a Millipore System equipped with a 0.22 μm filter. All solvents used were of spectroscopic grade.

4.2. Sample Preparation. *4.2.1. Synthesis of ω-mercaptoundecyl Bromoisobutyrate.* The ATRP initiator was synthesized following a previously reported procedure.[36] Briefly, a mixture of bromoisobutyryl bromide (4.3 M) and 4-dimethylaminopyridine (12 M) in 1 mL ice-cold dichloro-

methane (dry) was added dropwise to a solution containing pyridine (0.14 M) and 11-mercaptoundecanol (0.16 M) in 30 mL of dry dichloromethane at 0 °C and stirred for 1 h at such temperature, followed by 18 h of stirring at room temperature. Once the reaction was complete, the product was extracted with a mixture of water (30 mL) and toluene (15 mL), and the aqueous phase was further washed with toluene (2 × 30 mL). Upon extraction, the organic phase was evaporated under vacuum and the resulting crude was dissolved in diethyl ether (40 mL), washed with a saturated ammonium chloride solution (3 × 40 mL), and dried over magnesium sulfate. The organic phase was then evaporated under reduced pressure, and the resulting yellowish oil was purified by column chromatography (silica gel, neutral) using 2% triethylamine in hexane as a mobile phase. Finally, a colorless oil was obtained upon hexane evaporation and drying the product under reduced pressure overnight. The purity of the final product was confirmed by ^{1}H NMR (400 MHz, CDCl$_3$): 4.14 (t, *J* = 6.6, 2H, OCH$_2$), 2.51 (q, *J* = 7.5, 2H, SCH$_2$), 1.91 (s, 6H, CH$_3$), 1.57−1.68 (m, 4H, CH$_2$), 1.24−1.36 (m, 16H, CH$_2$).

4.2.2. GaAs Sample Preconditioning. Bare bulk GaAs (001) wafers (6 mm × 6 mm, double side polished) were prepared for functionalization by cleaning in independent subsequent baths of acetone, opti-clear, acetone, and isopropanol under sonication for 5 min in each solvent. The substrates were then etched to remove native oxides by submerging them in 28% ammonium hydroxide for 2 min, thoroughly rinsed with degassed ethanol, and immediately submerged in the corresponding thiol solution.

4.2.3. Method A. 4.1.3.1. Preparation of PEG–Mercaptoundecanoic Acid-Functionalized GaAs (A–MUA–PEG). Immediately after etching, GaAs wafers were immersed in a 2 mM MUA solution in degassed ethanol and stirred for 24 h in order to form the corresponding mercaptoundecanoic (MUA−SAM). Upon incubation, the samples were thoroughly washed with ethanol and water and dried under a stream of Argon. Upon SAM formation, MUA-functionalized samples were immersed in a solution containing EDC (0.64 M) and NHS (0.13 M) in MES buffer (0.1 M, pH 4.7) and incubated for 2 h. Finally, the wafers were thoroughly washed with MES buffer, followed by their overnight incubation in a PEG diamine solution in MES buffer, rinsed with MES buffer, and dried under Argon.

4.2.4. Method B. 4.1.3.2. Preparation of Polyethylene Glycol–Mercaptoundecanoic Acid-Functionalized GaAs (B–MUA–PEG). Immediately after etching, GaAs wafers were immersed in a 2 mM MUA solution in degassed ethanol and stirred for 4 h, followed by an additional 16 h in static conditions in order to form the corresponding MUA−SAM. Upon SAM formation, MUA functionalized samples were immersed in an amine coupling solution (0.4 M EDC/0.1 M NHS in DI water) for 30 min and incubated for 30 min. Finally, the wafers were thoroughly washed with deionized water followed by their overnight incubation in a PEG diamine solution in dimethylformamide, rinsed with DMF, and dried under Nitrogen.

4.2.5. Preparation of GMA PBs on GaAs (MUBIB–Ep) through ATRP. Etched GaAs wafers were immersed in a 2 mM MUBIB solution in degassed ethanol and stirred for 24 h. Upon incubation, the samples were thoroughly washed with ethanol and water and dried under a stream of Argon in order to form the corresponding MUBIB self-assembled monolayer

(MUBIB−SAM). Upon SAM formation, MUBIB−Ep wafers were obtained by following a slightly modified procedure of MUBIB−Ep deposition on initiator-activated glass substrates.[19] Briefly, MUBIB (SAM) samples were immersed in a solution containing 2,2-bipyridyl (Bipy, 30 mM), CuBr$_2$ (15 mM), and GMA (2%, v/v) in methanol/water (1:1 v/v). Right before polymerization, ascorbic acid was rapidly added (13.5 mM) into the polymerization solution followed by the immediate capping of the vials and incubation for 2 h under agitation. Finally, the samples were removed from the polymerization solution, rinsed thoroughly with 1:1 methanol/water, and dried under a stream of Nitrogen.

4.2.6. Incorporation of Phenylboronic Acid Moieties to MUBIB−Ep (MUBIB−Ep−PhB). MUBIB−Ep−PhB was prepared following a procedure previously reported where MUBIB−Ep was deposited on initiator-activated glass substrates.[30] Briefly, MUBIB−Ep wafers were immersed in a solution containing 3-aminophenylboronic acid (50 mM) in methanol/water (1:1, v/v) followed by incubation for 1 h at room temperature under agitation. Finally, the obtained samples were removed from the solution, thoroughly washed with 1:1 methanol/water, and dried under a stream of Argon.

4.2.7. Incorporation of Polyethylene Glycol Diamine Moieties to MUBIB−Ep (MUBIB−Ep−PEG). MUBIB−Ep−PEG wafers were prepared following a part of PEG PBs immobilization on glass-type surfaces.[37] Briefly, pure and dry PEG diamine (MW 2000) was directly deposited on MUBIB−Ep followed by incubation at 75 °C for 36 h. The obtained samples were then thoroughly washed with water and methanol and dried under a stream of Argon.

4.3. Antibody Grafting Experiments. *4.3.1. Grafting of IgG-anti E. coli and L. pneumophila Antibodies onto MUA−PEG (MUA−PEG−Ab).* Antibody incorporation on MUA−PEG wafers was performed by incubating the samples overnight in a 5 M glutaric anhydride solution in DMF with the purpose of transforming PEG amino groups into carboxylic acids. Then, the samples were incubated separately in an amine coupling solution for 0.5 h. Antibody grafting was achieved by sample incubation in a 100 μg/mL solution of unconjugated IgG-anti *L. pneumophila* antibodies in PBS buffer (1×), followed by rinsing the substrates with PBS buffer and drying under an Argon flow. As a final treatment, nonspecific interactions were minimized by incubating the samples in a 2% BSA solution in PBS buffer for 0.5 h and by incubation for another 0.5 h in 1 M ethanolamine solution (pH 8) for 0.5 h in 1 M ethanolamine solution (pH 8).

4.3.2. Grafting of IgG-anti E coli and L. pneumophila Antibodies onto MUBIB−Ep−PhB (MUBIB−Ep−PhB−Ab. MUBIB−Ep−PhB samples were incubated for 1 h in a 100 μg/mL unconjugated IgG-anti *L. pneumophila* solution in PBS. As a final treatment, nonspecific interactions were minimized by two consecutive blocking steps using a 2% BSA solution in PBS buffer for 0.5 h and by incubation for another 0.5 h in 1 M ethanolamine solution (pH 8).

4.3.3. Grafting of IgG-anti E. coli and L. pneumophila Antibodies onto MUBIB−Ep−PEG (MUBIB−Ep−PEG−Ab). Antibody incorporation on MUBIB−Ep−PEG substrates was performed by separately activating the antibodies' carboxylic groups by incubating in a solution containing EDC (0.64 M) and NHS (0.13 M) in 0.1 M MES buffer at pH 4.5 for 2 h. Then, MUBIB−Ep−PEG substrates were immersed for 1 h in a 100 μg/mL unconjugated IgG-anti *L. pneumophila* solution in PBS. As a final treatment, nonspecific interactions were

minimized by incubating the samples in a 2% BSA solution in PBS buffer for 0.5 h and by incubation for another 0.5 h in 1 M ethanolamine solution (pH 8) for 0.5 h in 1 M ethanolamine solution (pH 8).

4.3.4. Bacteria Capture Experiments. Antibody-functionalized substrates were incubated in suspensions of 10^5 CFU mL^{-1} and 10^3 CFU mL^{-1} of green fluorescent protein-labeled *E. coli* prepared in 1× PBS (pH 7.4) obtained, following dilution of a freshly prepared culture in LB. Upon incubation, the substrates were rinsed three times with 1× PBS (pH 7.4) and deionized water.

4.4. Sample Characterization. *4.4.1. Ellipsometry.* Film thickness measurements were performed using a Plasmos SD2000 single wavelength (632 nm) multiangle ellipsometer.

4.4.2. Contact Angle. Static contact angle measurements were performed with a goniometer equipped with a CCD camera (iuVCR software). High purity deionized water (resistivity 18 MΩ·cm^{-1}) was used, and a drop volume was approximately at 5 μL. The average contact angle values were estimated in the drop analysis module from ImageJ software.

4.4.3. FTIR Spectroscopy. FTIR transmission spectra of functionalized GaAs samples with PBs were recorded with a Bruker Vertex 70v spectrometer equipped with a RockSolid interferometer and a wide-range Globar IR source covering 6000 to 50 cm^{-1}. The signal was collected with a liquid nitrogen-cooled MCT (mercury cadmium telluride) IR detector. The spectral resolution was set to 4 cm^{-1}, all measurements were carried out under vacuum, and spectra were collected with 256 scans and by using an aperture of 1.5 mm. The spectrum of an etched GaAs (100) sample was used as a blank and subtracted from SAM spectra.

4.4.4. Atomic Force Microscopy. High-resolution imaging was carried out with an atomic force microscope (AFM, Veeco Dimension 3000) under air, using tapping mode. The AFM cantilever had a nominal resonance frequency of 330 kHz, force constant of 42 N/m, a length of 125 μm, and a mean width of 30 μm. Scans of different dimensions were recorded in order to have a representative sampling of the surface.

4.4.5. Fluorescence Microscopy. Fluorescence-labeled antibody and GFP *E. coli* coverage was recorded using an Olympus IX71 fluorescence microscope. Six to eight images were taken per sample at different sample sites with a magnification of 20× using the fluorescein isothiocyanate (FITC) filter, providing excitation and emission wavelengths of approximately 495/519 nm. The number of antibodies was determined following an ImageJ protocol for antibody counting.

4.4.6. X-ray Photoelectron Spectroscopy. XPS was performed by using a Kratos analytical model Axis Ultra DLD, using monochromatic aluminum Ka X-rays at 140 W. XPS data were analyzed using CASAXPS software.

■ ASSOCIATED CONTENT

ⓢ Supporting Information

The Supporting Information is available free of charge at https://pubs.acs.org/doi/10.1021/acsomega.0c04954.

> Details of PBs methodologies employed in this work and those applied by others as a reference to the technology of GaAs-based biosensors and PB−GaAs interface (PDF)

AUTHOR INFORMATION

Corresponding Authors

Maria C. DeRosa − *Department of Chemistry, Carleton University, Ottawa, Ontario K1S 5B6, Canada;* orcid.org/0000-0003-1868-6357; Email: MariaDerosa@cunet.carleton.ca

Jan J. Dubowski − *Interdisciplinary Institute for Technological Innovation (3IT), CNRS UMI-3463, Université de Sherbrooke, Sherbrooke, Québec J1K 0A5, Canada;* orcid.org/0000-0003-0022-527X; Email: Jan.J.Dubowski@USherbrooke.ca

Authors

Daniela T. Marquez − *Interdisciplinary Institute for Technological Innovation (3IT), CNRS UMI-3463, Université de Sherbrooke, Sherbrooke, Québec J1K 0A5, Canada; Department of Chemistry, Carleton University, Ottawa, Ontario K1S 5B6, Canada*

Juliana Chawich − *Interdisciplinary Institute for Technological Innovation (3IT), CNRS UMI-3463, Université de Sherbrooke, Sherbrooke, Québec J1K 0A5, Canada*

Walid M. Hassen − *Interdisciplinary Institute for Technological Innovation (3IT), CNRS UMI-3463, Université de Sherbrooke, Sherbrooke, Québec J1K 0A5, Canada*

Khalid Moumanis − *Interdisciplinary Institute for Technological Innovation (3IT), CNRS UMI-3463, Université de Sherbrooke, Sherbrooke, Québec J1K 0A5, Canada*

Complete contact information is available at:
https://pubs.acs.org/10.1021/acsomega.0c04954

Notes

The authors declare no competing financial interest.

REFERENCES

(1) Ahmed, A.; Rushworth, J. V.; Hirst, N. A.; Millner, P. A. Biosensors for Whole-Cell Bacterial Detection. *Clin. Microbiol. Rev.* **2014**, *27*, 631−646.

(2) Aziziyan, M. R.; Hassen, W. M.; Morris, D.; Frost, E. H.; Dubowski, J. J. Photonic Biosensor Based on Photocorrosion of GaAs/AlGaAs Quantum Heterostructures for Detection of Legionella Pneumophila. *Biointerphases* **2016**, *11*, 019301.

(3) Nazemi, E.; Hassen, W. M.; Frost, E. H.; Dubowski, J. J. Monitoring Growth and Antibiotic Susceptibility of Escherichia Coli with Photoluminescence of GaAs/AlGaAs Quantum Well Microstructures. *Biosens. Bioelectron.* **2017**, *93*, 234−240.

(4) Nazemi, E.; Aithal, S.; Hassen, W. M.; Frost, E. H.; Dubowski, J. J. GaAs/AlGaAs Heterostructure Based Photonic Biosensor for Rapid Detection of Escherichia Coli in Phosphate Buffered Saline Solution. *Sens. Actuators, B* **2015**, *207*, 556−562.

(5) Islam, M. A.; Hassen, W. M.; Tayabali, A. F.; Dubowski, J. J. Antimicrobial Warnericin RK Peptide Functionalized GaAs/AlGaAs Biosensor for Highly Sensitive and Selective Detection of Legionella Pneumophila. *Biochem. Eng. J.* **2020**, *154*, 107435.

(6) Chen, W.-L.; Cordero, R.; Tran, H.; Ober, C. K. 50th Anniversary Perspective: Polymer Brushes: Novel Surfaces for Future Materials. *Macromolecules* **2017**, *50*, 4089−4113.

(7) Kim, M.; Schmitt, S.; Choi, J.; Krutty, J.; Gopalan, P. From Self-Assembled Monolayers to Coatings: Advances in the Synthesis and Nanobio Applications of Polymer Brushes. *Polymers* **2015**, *7*, 1346−1378.

(8) Krishnamoorthy, M.; Hakobyan, S.; Ramstedt, M.; Gautrot, J. E. Surface-Initiated Polymer Brushes in the Biomedical Field: Applications in Membrane Science, Biosensing, Cell Culture, Regenerative Medicine and Antibacterial Coatings. *Chem. Rev.* **2014**, *114*, 10976−11026.

(9) Kaholek, M.; Lee, W.-K.; LaMattina, B.; Caster, K. C.; Zauscher, S. Fabrication of Stimulus-Responsive Nanopatterned Polymer Brushes by Scanning-Probe Lithography. *Nano Lett.* **2004**, *4*, 373−376.

(10) Seifert, M.; Koch, A. H. R.; Deubel, F.; Simmet, T.; Hess, L. H.; Stutzmann, M.; Jordan, R.; Garrido, J. A.; Sharp, I. D. Functional Polymer Brushes on Hydrogenated Graphene. *Chem. Mater.* **2013**, *25*, 466−470.

(11) Steenackers, M.; Sharp, I. D.; Larsson, K.; Hutter, N. A.; Stutzmann, M.; Jordan, R. Structured Polymer Brushes on Silicon Carbide. *Chem. Mater.* **2010**, *22*, 272−278.

(12) Ye, Y.; Chen, L.; Krull, U. J. Light Induced Surface Corrosion of Gallium Arsenide for Immobilization of Oligonucleotide Probes. *Anal. Lett.* **2008**, *41*, 289−301.

(13) Dubowski, J. J.; Voznyy, O.; Marshall, G. M. Molecular Self-Assembly and Passivation of GaAs (001) with Alkanethiol Monolayers: A View towards Bio-Functionalization. *Appl. Surf. Sci.* **2010**, *256*, 5714−5721.

(14) Tkachev, M.; Anand-Kumar, T.; Bitler, A.; Guliamov, R.; Naaman, R. Enabling Long-Term Operation of GaAs-Based Sensors. *Engineering* **2013**, *05*, 1−12.

(15) Tang, L.; Chun, I. S.; Wang, Z.; Li, J.; Li, X.; Lu, Y. DNA Detection Using Plasmonic Enhanced Near-Infrared Photoluminescence of Gallium Arsenide. *Anal. Chem.* **2013**, *85*, 9522−9527.

(16) Cai, Q. J.; Fu, G. D.; Zu, F. R.; Kang, E.-T.; Neoh, K.-G. GaAs−Polymer Hybrids Formed by Surface-Initiated Atom-Transfer Radical Polymerization of Methyl Methacrylate. *Angew. Chem., Int. Ed.* **2005**, *44*, 1104−1107.

(17) McGuiness, C. L.; Diehl, G. A.; Blasini, D.; Smilgies, D.-M.; Zhu, M.; Samarth, N.; Weidner, T.; Ballav, N.; Zharnikov, M.; Allara, D. L. Molecular Self-Assembly at Bare Semiconductor Surfaces: Cooperative Substrate−Molecule Effects in Octadecanethiolate Monolayer Assemblies on GaAs(111), (110), and (100). *ACS Nano* **2010**, *4*, 3447−3465.

(18) Baum, T.; Ye, S.; Uosaki, K. Formation of Self-Assembled Monolayers of Alkanethiols on GaAs Surface with in Situ Surface Activation by Ammonium Hydroxide. *Langmuir* **1999**, *15*, 8577−8579.

(19) Ye, S.; Li, G.; Noda, H.; Uosaki, K.; Osawa, M. Characterization of Self-Assembled Monolayers of Alkanethiol on GaAs Surface by Contact Angle and Angle-Resolved XPS Measurements. *Surf. Sci.* **2003**, *529*, 163−170.

(20) Huang, X.; Dubowski, J. J. Solvent-Mediated Self-Assembly of Hexadecanethiol on GaAs (001). *Appl. Surf. Sci.* **2014**, *299*, 66−72.

(21) McGuiness, C. L.; Shaporenko, A.; Zharnikov, M.; Walker, A. V.; Allara, D. L. Molecular Self-Assembly at Bare Semiconductor Surfaces: Investigation of the Chemical and Electronic Properties of the Alkanethiolate−GaAs(001) Interface. *J. Phys. Chem. C* **2007**, *111*, 4226−4234.

(22) Abrahamsson, S.; Dahlen, B.; Löfgren, H.; Pascher, I. Lateral Packing of Hydrocarbon Chains. *Prog. Chem. Fats Other Lipids* **1978**, *16*, 125−143.

(23) Lilge, I.; Steuber, M.; Tranchida, D.; Sperotto, E.; Schönherr, H. Tailored (Bio)Interfaces via Surface Initiated Polymerization: Control of Grafting Density and New Responsive Diblock Copolymer Brushes. *Macromol. Symp.* **2013**, *328*, 64−72.

(24) Aziziyan, M. R.; Sharma, H.; Dubowski, J. J. Photo-Atomic Layer Etching of GaAs/AlGaAs Nanoheterostructures. *ACS Appl. Mater. Interfaces* **2019**, *11*, 17968−17978.

(25) Huang, X.; Liu, N.; Moumanis, K.; Dubowski, J. J. Water-Mediated Self-Assembly of 16-Mercaptohexadecanoic Acid on GaAs (001). *J. Phys. Chem. C* **2013**, *117*, 15090−15097.

(26) Zhuang, P.; Dirani, A.; Glinel, K.; Jonas, A. M. Temperature Dependence of the Surface and Volume Hydrophilicity of Hydrophilic Polymer Brushes. *Langmuir* **2016**, *32*, 3433−3444.

(27) Ulman, A. Formation and Structure of Self-Assembled Monolayers. *Chem. Rev.* **1996**, *96*, 1533−1554.

(28) De Morais, L. C.; Bernardes-Filho, R.; Assis, O. B. G. Wettability and Bacteria Attachment Evaluation of Multilayer Proteases Films for Biosensor Application. *World J. Microbiol. Biotechnol.* **2009**, *25*, 123−129.

(29) Lorenzetti, M.; Dogša, I.; Stošicki, T.; Stopar, D.; Kalin, M.; Kobe, S.; Novak, S. The Influence of Surface Modification on Bacterial Adhesion to Titanium-Based Substrates. *ACS Appl. Mater. Interfaces* **2015**, *7*, 1644−1651.

(30) Liu, Y.; Zhang, Y.; Zhao, Y.; Yu, J. Phenylboronic Acid Polymer Brush-Enabled Oriented and High Density Antibody Immobilization for Sensitive Microarray Immunoassay. *Colloids Surf., B* **2014**, *121*, 21−26.

(31) Ma, R.; Yang, H.; Li, Z.; Liu, G.; Sun, X.; Liu, X.; An, Y.; Shi, L. Phenylboronic Acid-Based Complex Micelles with Enhanced Glucose-Responsiveness at Physiological PH by Complexation with Glycopolymer. *Biomacromolecules* **2012**, *13*, 3409−3417.

(32) Sauer-Budge, A. F.; Boardman, A. K.; Allison, S.; Wirz, H.; Foss, D.; Sharon, A. Materials and Surface Properties Optimization to Prevent Biofouling of a Novel Bacterial Concentrator. *Procedia CIRP* **2013**, *5*, 185−188.

(33) Vashist, S. K.; Dixit, C. K.; Maccraith, B. D.; O'Kennedy, R. Effect of Antibody Immobilization Strategies on the Analytical Performance of a Surface Plasmon Resonance-Based Immunoassay. *Analyst* **2011**, *136*, 4431−4436.

(34) Aziziyan, M. R.; Hassen, W. M.; Sharma, H.; Shirzaei Sani, E.; Annabi, N.; Frost, E. H.; Dubowski, J. J. Sodium Dodecyl Sulfate Decorated Legionella Pneumophila for Enhanced Detection with a GaAs/AlGaAs Nanoheterostructure Biosensor. *Sens. Actuators, B* **2020**, *304*, 127007.

(35) Hassen, W. M.; Sanyal, H.; Hammood, M.; Moumanis, K.; Frost, E. H.; Dubowski, J. J. Chemotaxis for Enhanced Immobilization of Escherichia Coli and Legionella Pneumophila on Biofunctionalized Surfaces of GaAs. *Biointerphases* **2016**, *11*, 021004.

(36) Wassel, E.; Jiang, S.; Song, Q.; Vogt, S.; Nöll, G.; Druzhinin, S. I.; Schönherr, H. Thickness Dependence of Bovine Serum Albumin Adsorption on Thin Thermoresponsive Poly(Diethylene Glycol) Methyl Ether Methacrylate Brushes by Surface Plasmon Resonance Measurements. *Langmuir* **2016**, *32*, 9360−9370.

(37) Piehler, J.; Brecht, A.; Valiokas, R.; Liedberg, B.; Gauglitz, G. A High-Density Poly(Ethylene Glycol) Polymer Brush for Immobilization on Glass-Type Surfaces. *Biosens. Bioelectron.* **2000**, *15*, 473−481.